Supplemental Figure Legends

Supplemental Figure 1. Expression of LMOD1 in embryonic human intestine. LMOD1 is expressed (brown stain) in smooth muscle cells that constitute layers of the intestine (**A-C**) and bladder (**D-F**), including muscularis mucosa, blood vessels, and both muscle layers of the muscularis propria. (**G**) Western blot showing LMOD1 expression in human aorta, bladder, and intestine, with undetectable expression in the kidney.

Supplemental Figure 2. CRISPR-Cas9 targeting of CArG elements at *Lmod1.* (**A**) Schematic of *Lmod1* proximal promoter (prom.) region containing two conserved CArG elements (vertical purple lines with indicated wild type sequences in black) showing position of gRNA (blue) immediately 5' of a PAM sequence (red) located within the more proximal CArG box. Guide-RNA (Supplemental Table 4), *Cas9* mRNA, and single-stranded repair template (Supplemental Table 4) were injected into mouse fertilized eggs. The single-stranded oligonucleotide used in homology-directed repair contained the green substituted nucleotides within each CArG box; the PAM sequence was not mutated. (**B**) Alignment of Sanger sequencing confirmed CArG box (yellow) mutations in CArG-Mut mice. PAM sequence is highlighted in red. (**C**) RT-qPCR showing reduced *Lmod1* expression in aorta of CArG-Mut mice, but no difference in other tissues. Average *Lmod1* Ct value indicated above each bar. (**D**) Western blot showing no significant difference in LMOD1, MYH11, or TAGLN protein in CArG-WT or CArG-Mut bladder tissue. (**E**) Quantitation of LMOD1 protein in aorta and bladder of CArG-WT and CArG-Mut mice. No significant decrease in LMOD1 protein was observed in either tissue. Error bars here and in panel C are standard deviations around the mean.

Supplemental Figure 3. Expression of SMC contractile proteins in *Lmod1* mutant mice. (A) Western blot of LMOD1 protein (upper band, arrow) expression in aorta of indicated genotypes. The lower band here and elsewhere is non-specific as evidenced by its presence in the knockout aorta. (**B**) Western blot showing LMOD1 expression levels in bladder tissue from wild type (+/+), heterozygous (+/-), compound heterozygous (one allele carrying the 151 bp deletion of exon one and the other allele harboring mutations in both CArG elements at the *Lmod1* promoter; MUT/-), or homozygous (-/-) deletion of *Lmod1*.

Supplemental Figure 4. Non-specific binding of LMOD1 antibody. (**A**) Immunofluorescence microscopy showing LMOD1 and ACTA2 in sections of bladder tissue from wild type (WT) control or *Lmod1*$^{-/-}$ knockout (KO) mice, stained with either anti-LMOD1 antibody or normal IgG control. Note persistent weak signal with IgG control antibody and the thinning of the epithelial lining (ACTA2 negative stain) in bladder of KO. (**B**) Western blot of stomach and bladder tissue from control and *Lmod1*$^{-/-}$ mice depicting lower molecular weight bands that are not specific for LMOD1. Such nonspecific binding likely underscores the weak staining seen in *Lmod1* knockout mouse tissues such as bladder in panel A above as well as in Figures 3, 4, and 5 of main text.

Supplemental Figure 5. Increased proliferation in outer SMC layer of intestine in *Lmod1* knockout. (**A**) Images of Ki-67 stained (green stain, white arrows) sections of intestine from *Lmod1*$^{-/-}$ and control mice. White arrowheads indicate an increase in Ki-67 positive cells in the outer SMC layer of *Lmod1*$^{-/-}$ intestine. Sections were counterstained with MYH11 (red). Images taken with 40X objective. (**B**) Quantification of Ki-67+ cells in outer and inner SMC layers of the intestine. * = p value < 0.05. n = 9 for +/+, n= 14 for -/-. (**C**) Immunofluoresence microscopy images showing no detectable differences in TUNEL staining between *Lmod1*$^{-/-}$ and wild type control mice. Positive control sample of intestine was subjected to DNase 1 treatment.

Supplemental Figure 6. *Lmod1* knockout results in shortened intestinal length. (**A**) Gross pathology of stomach and whole intestine from *Lmod1*$^{+/-}$ and *Lmod1*$^{-/-}$ mice. Note the distended stomach and shortened intestinal length in *Lmod1*$^{-/-}$ tissues. (**B**) Quantification of intestinal length from part A. *Lmod1* deletion results in significantly shorter intestinal length. (**C**) Quantification of colon diameter from H&E-stained sections from control and *Lmod1*$^{-/-}$ mice. Deletion of *Lmod1* did not result in the presence of a microcolon. Error bars are standard deviations around the means. All statistics calculated using unpaired Student T test, ** = p value < 0.01. (**D**) H&E-stained sections from control (a, c) and *Lmod1*$^{-/-}$ (b, d) mice of aorta (a, b) and esophagus (c, d) showing no overt histopathological changes with *Lmod1* deletion in these tissues.

Supplemental Figure 7. Human versus mouse LMOD1. CLUSTALW alignment of human versus mouse LMOD1 protein. Amino acid numbers for each species are shown at right. The colored and labeled boxed regions represent approximate locations of known functional domains in LMOD1. The mouse mutation introduced by two-component CRISPR editing is shown at top as a red boxed sequence labeled frameshift (fs) leading to a PTC (Stop sign; see also Figure 2C). The human point mutation is located further downstream and is indicated by a red box representing the SNP causing an Arginine (R) residue to become a PTC.

Supplemental Figure 8. *Lmod1* deletion results in decreased filamentous actin pelleted by ultracentrifugation. (**A**) In vivo G-actin:F-actin assay reveals that *Lmod1* deletion in primary mouse bladder tissue results in decreased levels of F-actin pelleted by ultracentrifugation (P). S and P refer to supernatant (G actin) and pellet (F-actin), respectively. (**B**) Quantification of *in vivo* G-actin:F-actin assay reveals that *Lmod1* deletion in primary mouse bladder tissue results in decreased levels of F-actin pelleted by ultracentrifugation**.** N = 7 for both knockout and control groups. Error bars represent the standard deviation around the mean. ** = p value < 0.01 using paired Student T test.

Supplemental Figure 9. *Lmod1* deletion results in decreased filamentous actin staining. Phalloidin staining (green) of duodenum and bladder from five control or five *Lmod1*$^{-/-}$ animals. Decreased phalloidin staining is consistently evident in *Lmod1*$^{-/-}$ bladder tissue.

Supplemental Figure 10. Transmission electron microscopy of dense bodies in *Lmod1*$^{-/-}$ bladder. Electron micrographs of dense bodies (black arrowheads) in smooth muscle of bladder (**a-c, e-**g) or intestine (**d, h)** tissue from *Lmod1*$^{-/-}$ (**a-d**) or *Lmod1*$^{+/+}$ (**e-h**) mice. Note abundance of glycogen granules (electron dense aggregates) in *Lmod1*$^{+/+}$ versus *Lmod1*$^{-/-}$. Scale bars are all 1 μm except for panel **c** which is 0.5 μm.

Supplemental Figure 11. Passive tension analysis of mouse jejunum ring segments and lack of compensation by other leiomodin proteins. (**A**) Myography data showing real-time measurements of passive tension in mouse jejunum ring segments. Tissues were mounted in PSS buffer and equilibrated at 37˚C for approximately 20 minutes prior to being dilated at regular intervals (black dotted lines), and the resulting passive tension was recorded approximately 1 minute later (time indicated by light blue lines on X axis). (**B**) RT-qPCR data showing no up-regulation of *Lmod2* or *Lmod3* in tissues following *Lmod1* deletion.

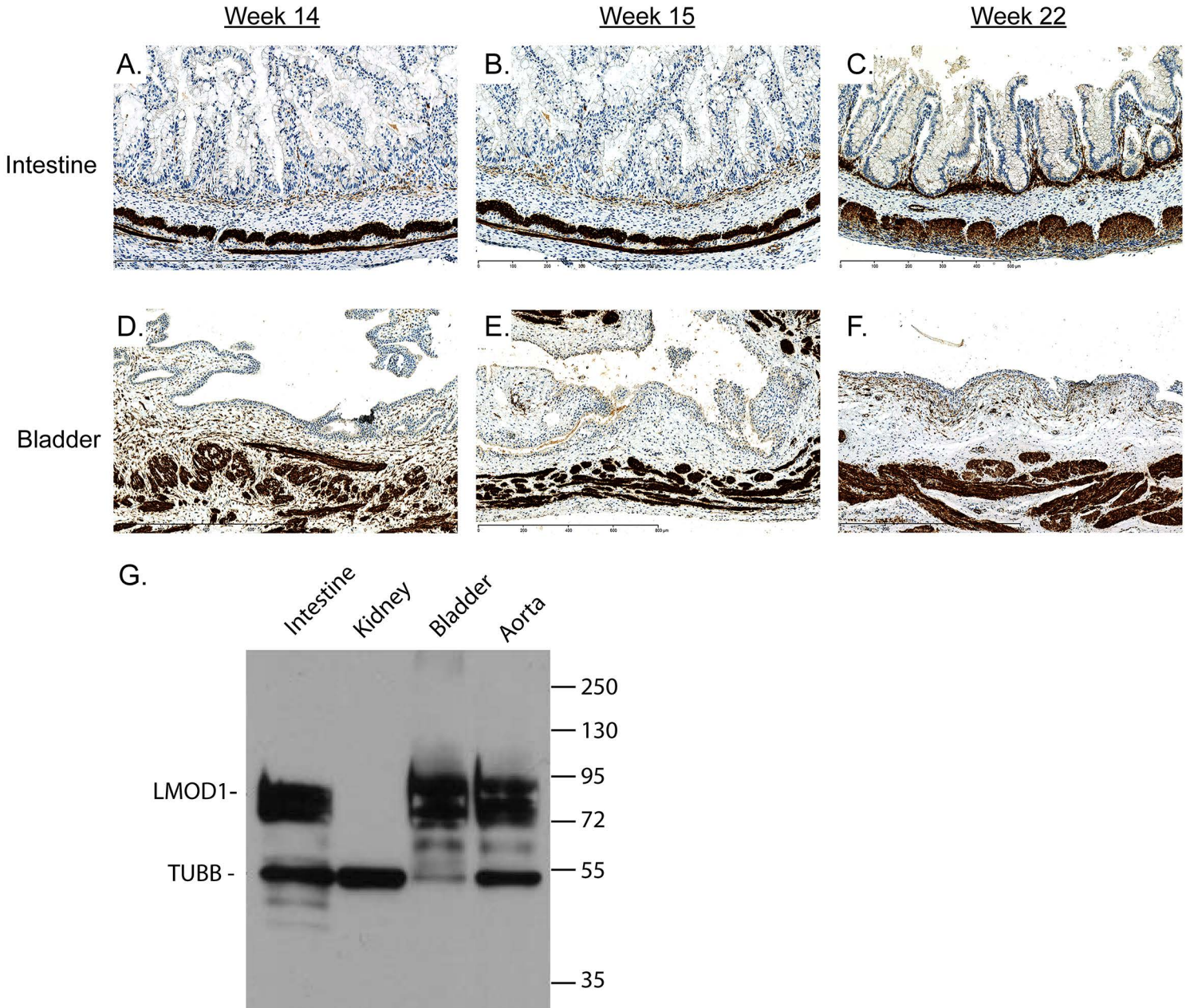
Week 14
Week 15
Week 22
A.
B.
C.
Intestine
D.
E.
F.
Bladder
G.
Intestine
Kidney
Bladder
Aorta
250
130
95
72
55
35
LMOD1-
TUBB -

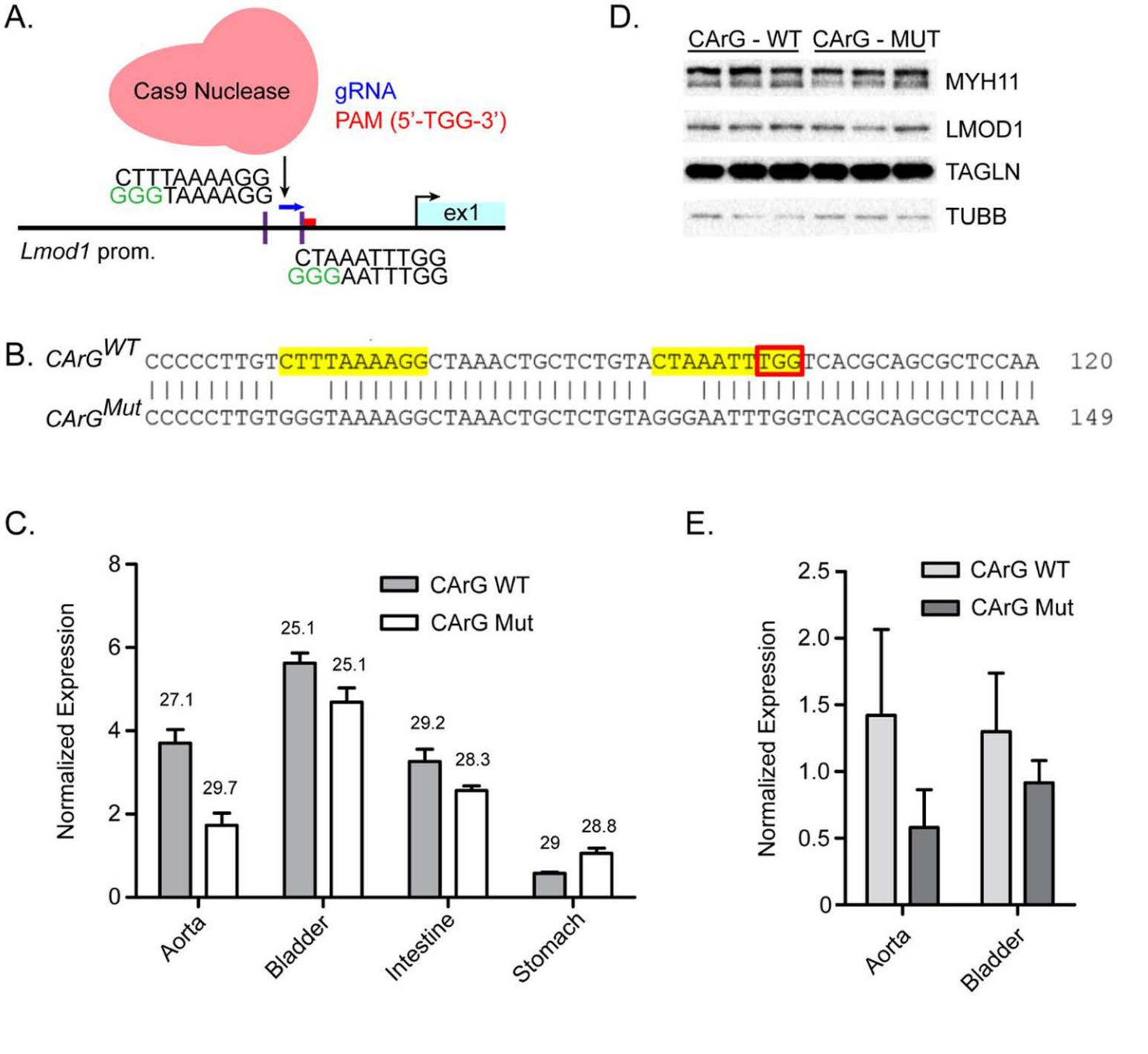
A.
Cas9 Nuclease
gRNA
PAM (5'-TGG-3')
CTTTAAAAGG
GGGTAAAAGG
ex1
Lmod1 prom.
CTAAATTTGG
GGGAATTTGG
D.
CArG - WT
CArG - MUT
MYH11
LMOD1
TAGLN
TUBB
B.
CArGWT CCCCCTTGTCTTTAAAAGGCTAAACTGCTCTGTACTAAATTTGGTCACGCAGCGCTCCAA 120
CArGMut CCCCCTTGTGGGTAAAAGGCTAAACTGCTCTGTAGGGAATTTGGTCACGCAGCGCTCCAA 149
C.
Normalized Expression
CArG WT
CArG Mut
27.1
29.7
25.1
25.1
29.2
28.3
29
28.8
Aorta
Bladder
Intestine
Stomach
E.
Normalized Expression
CArG WT
CArG Mut
Aorta
Bladder

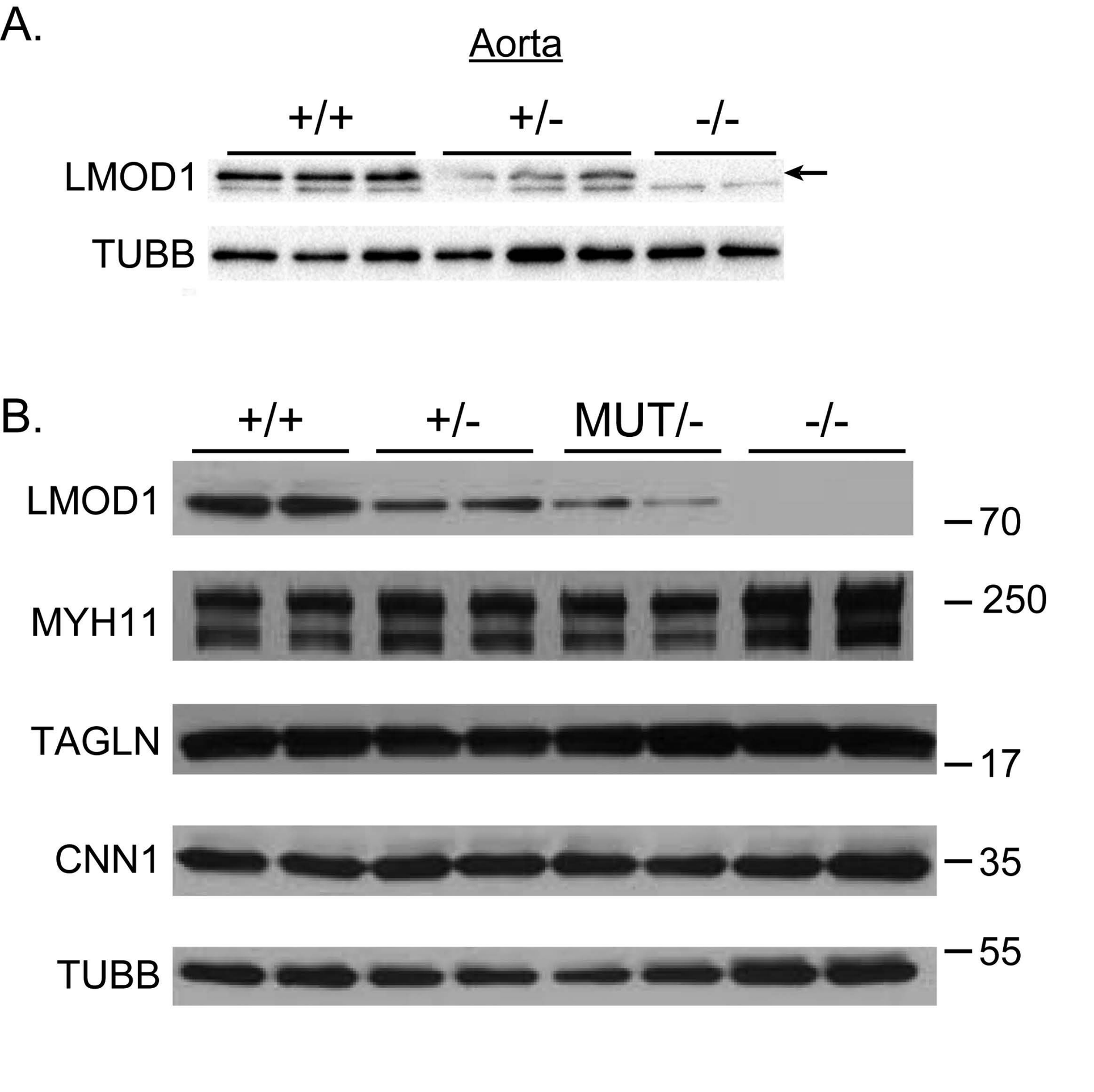
A.
Aorta
+/+
+/-
-/-
LMOD1
TUBB
B.
+/+
+/-
MUT/-
-/-
LMOD1
MYH11
TAGLN
CNN1
TUBB
70
250
17
35
55

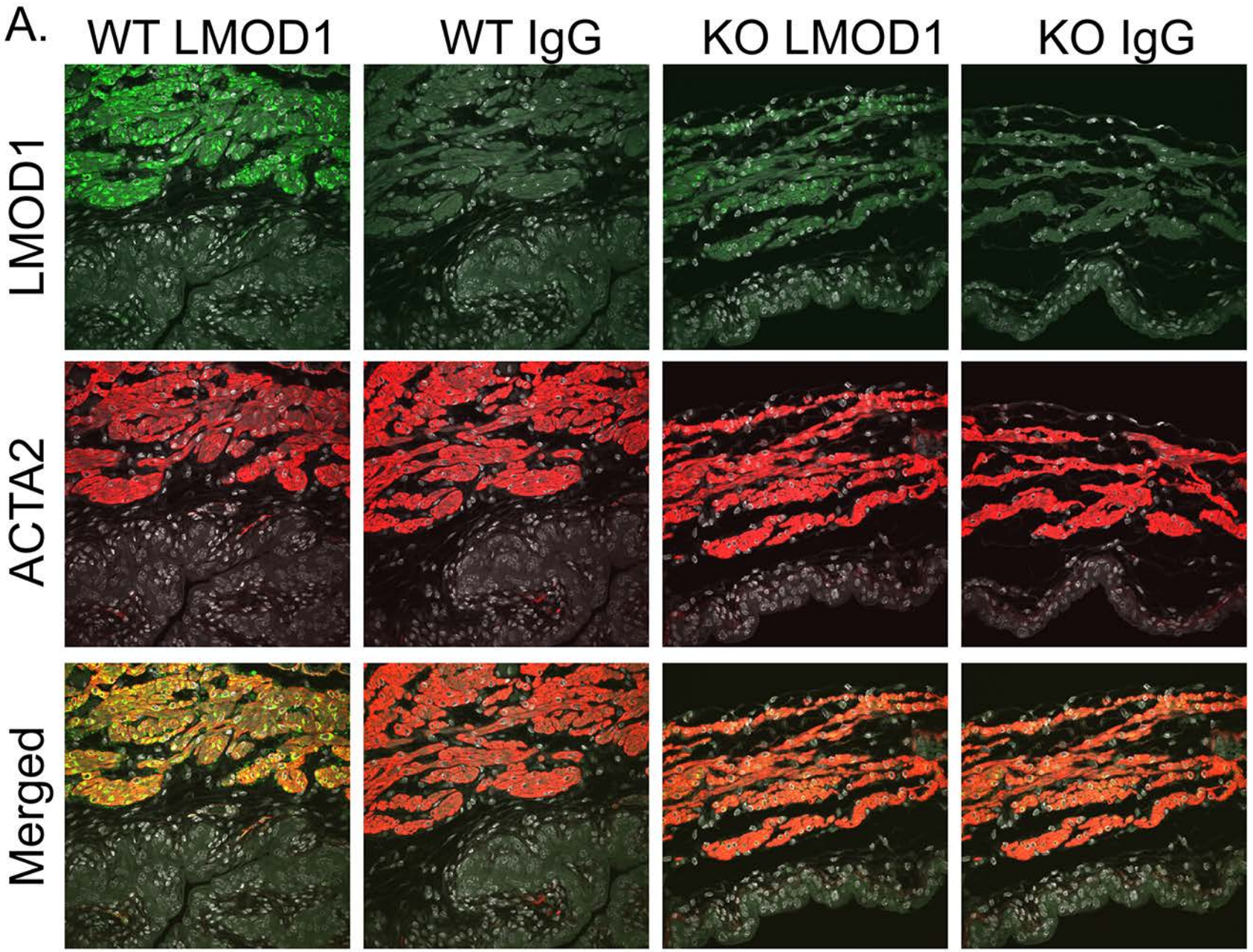
A.
WT LMOD1
WT IgG
KO LMOD1
KO IgG
LMOD1
ACTA2
Merged

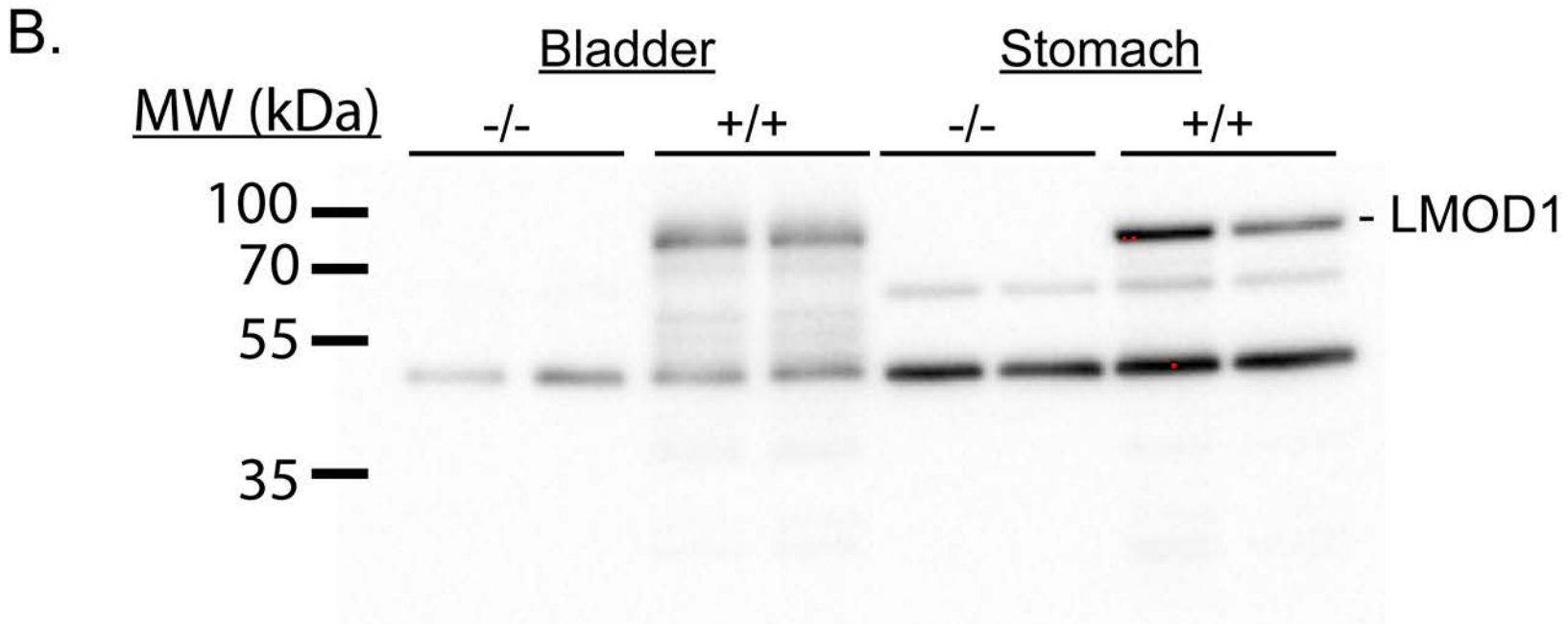
B.
Bladder
Stomach
MW (kDa)
-/-
+/+
-/-
+/+
100
70
55
35
- LMOD1

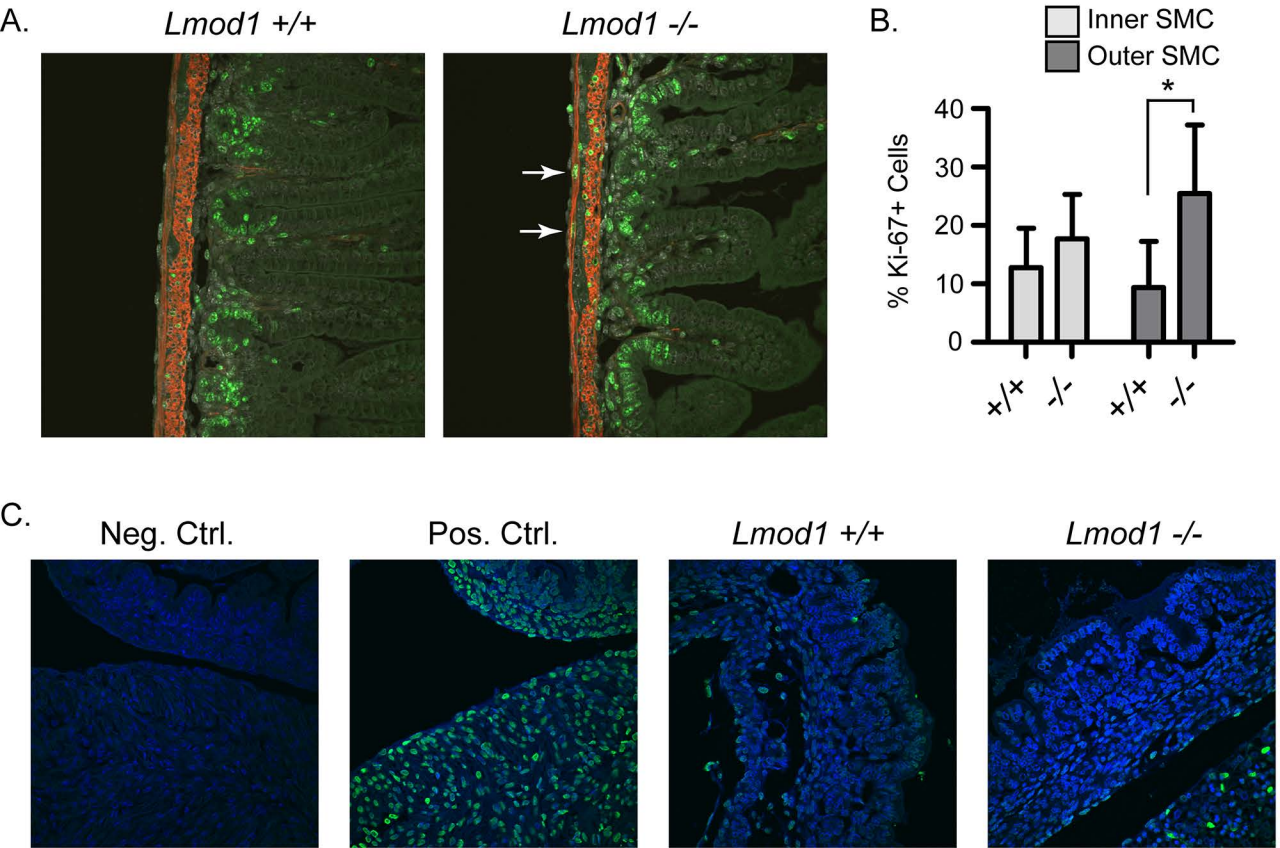
A.
Lmod1 +/+
Lmod1 -/-
B.
Inner SMC
Outer SMC
*
% Ki-67+ Cells
40
30
20
10
0
+/+
-/-
+/+
-/-
C.
Neg. Ctrl.
Pos. Ctrl.
Lmod1 +/+
Lmod1 -/-

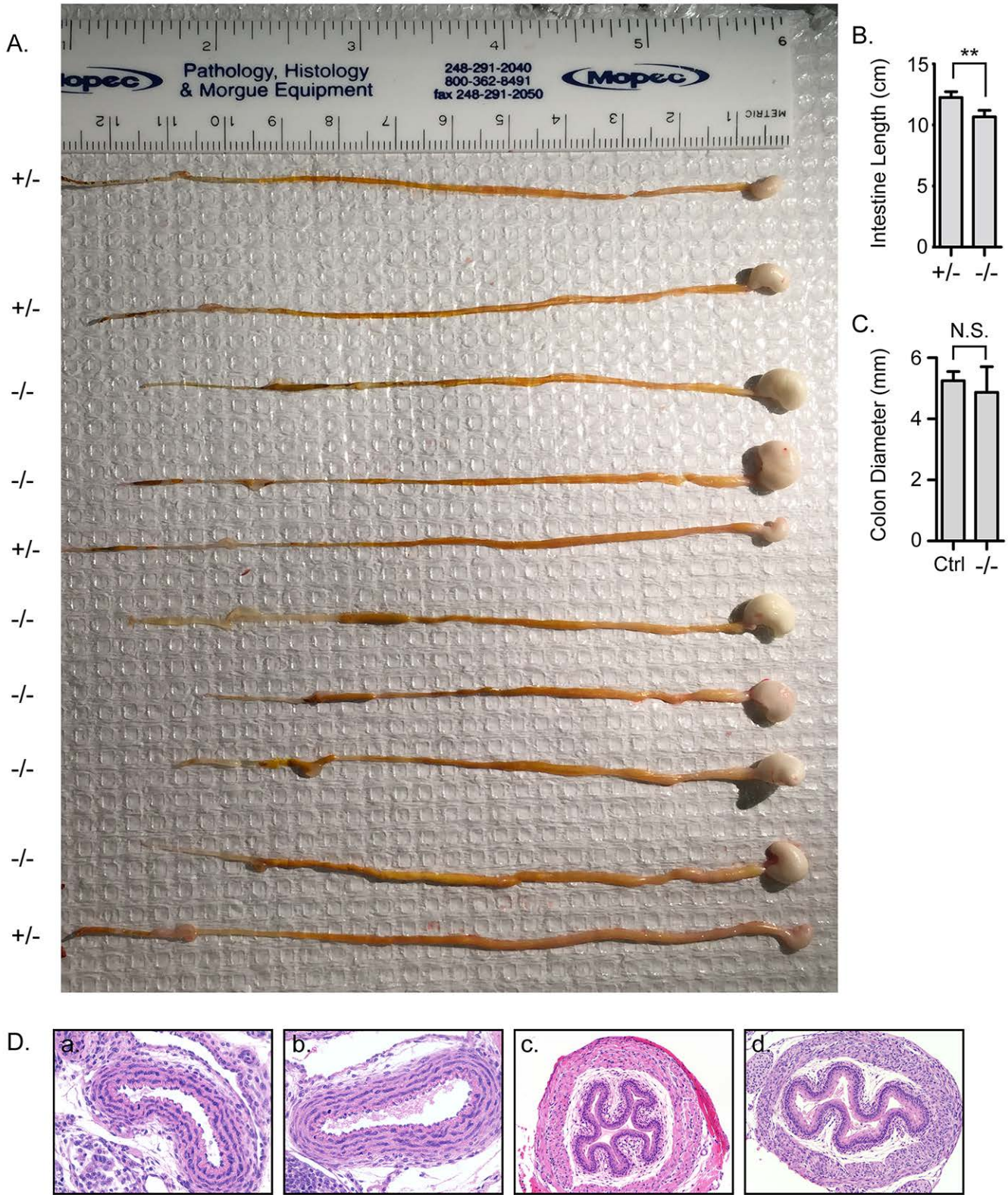
A.
Pathology, Histology
& Morgue Equipment
248-291-2040
800-362-8491
fax 248-291-2050
Mopec
+/-
+/-
-/-
-/-
+/-
-/-
-/-
-/-
-/-
+/-
B.
Intestine Length (cm)
**
15
10
5
0
+/-
-/-
C.
Colon Diameter (mm)
N.S.
6
4
2
0
Ctrl
-/-
D.
a.
b.
c.
d.

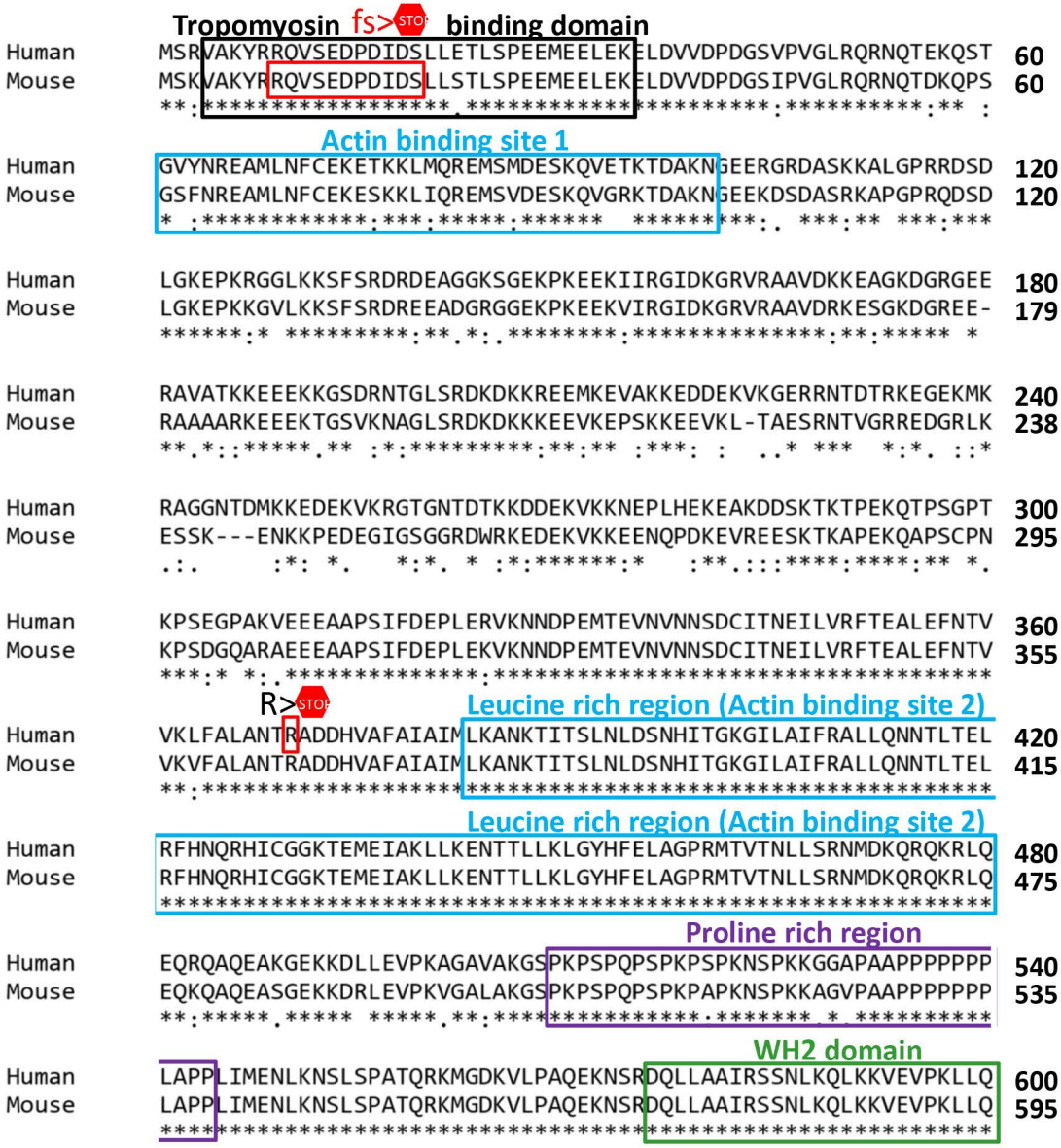
Tropomyosin
fs>STOP
binding domain
Human MSRVAKYRRQVSEDPDIDSLLETLSPEEMEELEKELDVVDPDGSVPVGLRQRNQTEKQST 60
Mouse MSKVAKYRRQVSEDPDIDSLLSTLSPEEMEELEKELDVVDPDGSIPVGLRQRNQTDKQPS 60
Actin binding site 1
Human GVYNREAMLNFCEKETKKLMQREMSMDESKQVETKTDAKNGEERGRDASKKALGPRRDSD 120
Mouse GSFNREAMLNFCEKESKKLIQREMSVDESKQVGRKTDAKNGEEKDSDASRKAPGPRQDSD 120
Human LGKEPKRGGLKKSFSRDRDEAGGKSGEKPKEEKIIRGIDKGRVRAAVDKKEAGKDGRGEE 180
Mouse LGKEPKKGVLKKSFSRDREEADGRGGEKPKEEKVIRGIDKGRVRAAVDRKESGKDGREE- 179
Human RAVATKKEEEKKGSDRNTGLSRDKDKKREEMKEVAKKEDDEKVKGERRNTDTRKEGEKMK 240
Mouse RAAAARKEEEKTGSVKNAGLSRDKDKKKEEVKEPSKKEEVKL-TAESRNTVGRREDGRLK 238
Human RAGGNTDMKKEDEKVKRGTGNTDTKKDDEKVKKNEPLHEKEAKDDSKTKTPEKQTPSGPT 300
Mouse ESSK---ENKKPEDEGIGSGGRDWRKEDEKVKKEENQPDKEVREESKTKAPEKQAPSCPN 295
Human KPSEGPAKVEEEAAPSIFDEPLERVKNNDPEMTEVNVNNSDCITNEILVRFTEALEFNTV 360
Mouse KPSDGQARAEEEAAPSIFDEPLEKVKNNDPEMTEVNVNNSDCITNEILVRFTEALEFNTV 355
R>STOP
Leucine rich region (Actin binding site 2)
Human VKLFALANTRADDHVAFAIAIMLKANKTITSLNLDSNHITGKGILAIFRALLQNNTLTEL 420
Mouse VKVFALANTRADDHVAFAIAIMLKANKTITSLNLDSNHITGKGILAIFRALLQNNTLTEL 415
Leucine rich region (Actin binding site 2)
Human RFHNQRHICGGKTEMEIAKLLKENTTLLKLGYHFELAGPRMTVTNLLSRNMDKQRQKRLQ 480
Mouse RFHNQRHICGGKTEMEIAKLLKENTTLLKLGYHFELAGPRMTVTNLLSRNMDKQRQKRLQ 475
Proline rich region
Human EQRQAQEAKGEKKDLLEVPKAGAVAKGSPKPSPQPSPKPSPKNSPKKGGAPAAPPPPPPP 540
Mouse EQKQAQEASGEKKDRLEVPKVGALAKGSPKPSPQPSPKPAPKNSPKKAGVPAAPPPPPPP 535
WH2 domain
Human LAPPLIMENLKNSLSPATQRKMGDKVLPAQEKNSRDQLLAAIRSSNLKQLKKVEVPKLLQ 600
Mouse LAPPLIMENLKNSLSPATQRKMGDKVLPAQEKNSRDQLLAAIRSSNLKQLKKVEVPKLLQ 595

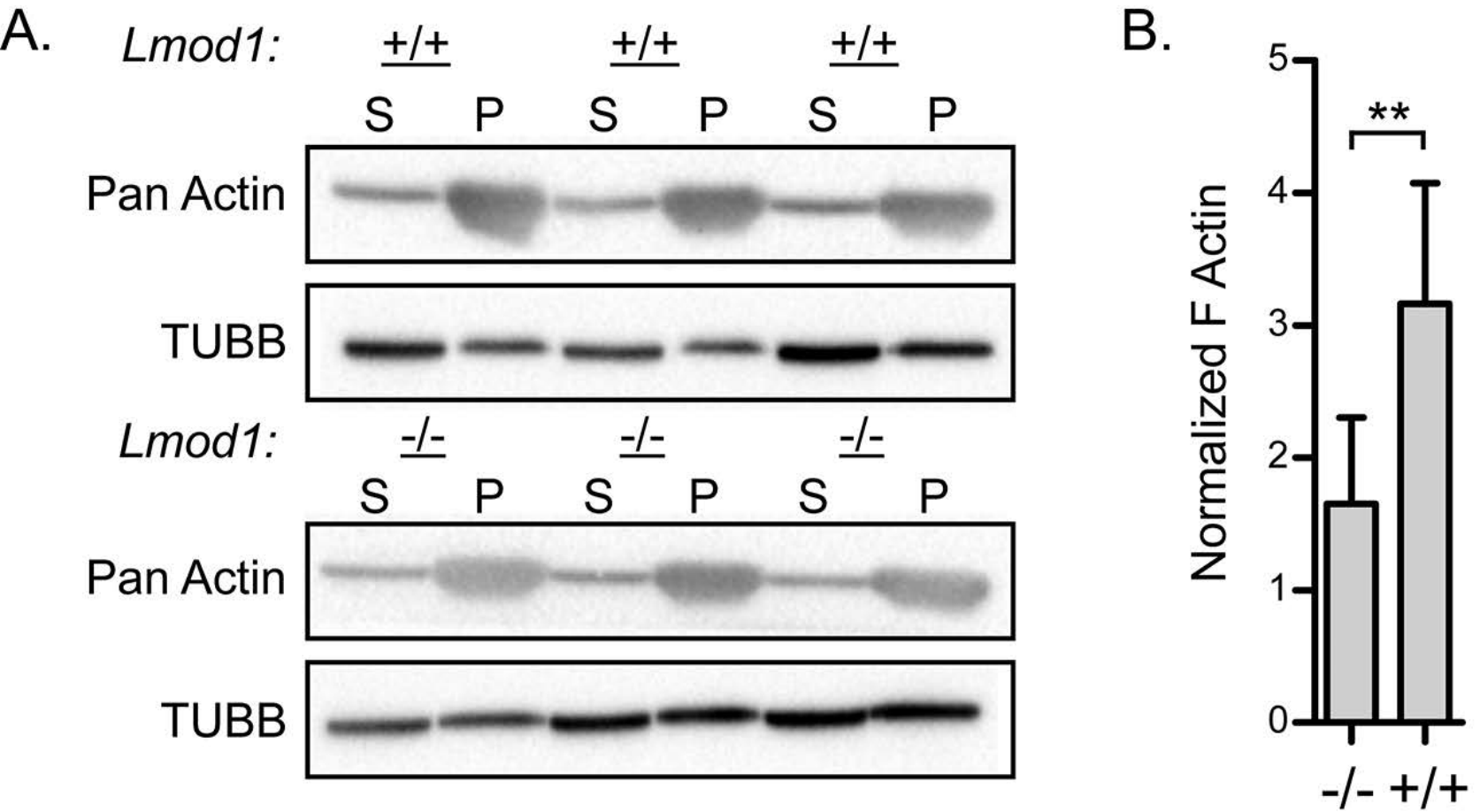
A.
Lmod1:
+/+
+/+
+/+
S
P
S
P
S
P
Pan Actin
TUBB
Lmod1:
-/-
-/-
-/-
S
P
S
P
S
P
Pan Actin
TUBB
B.
Normalized F Actin
5
4
3
2
1
0
**
-/-
+/+

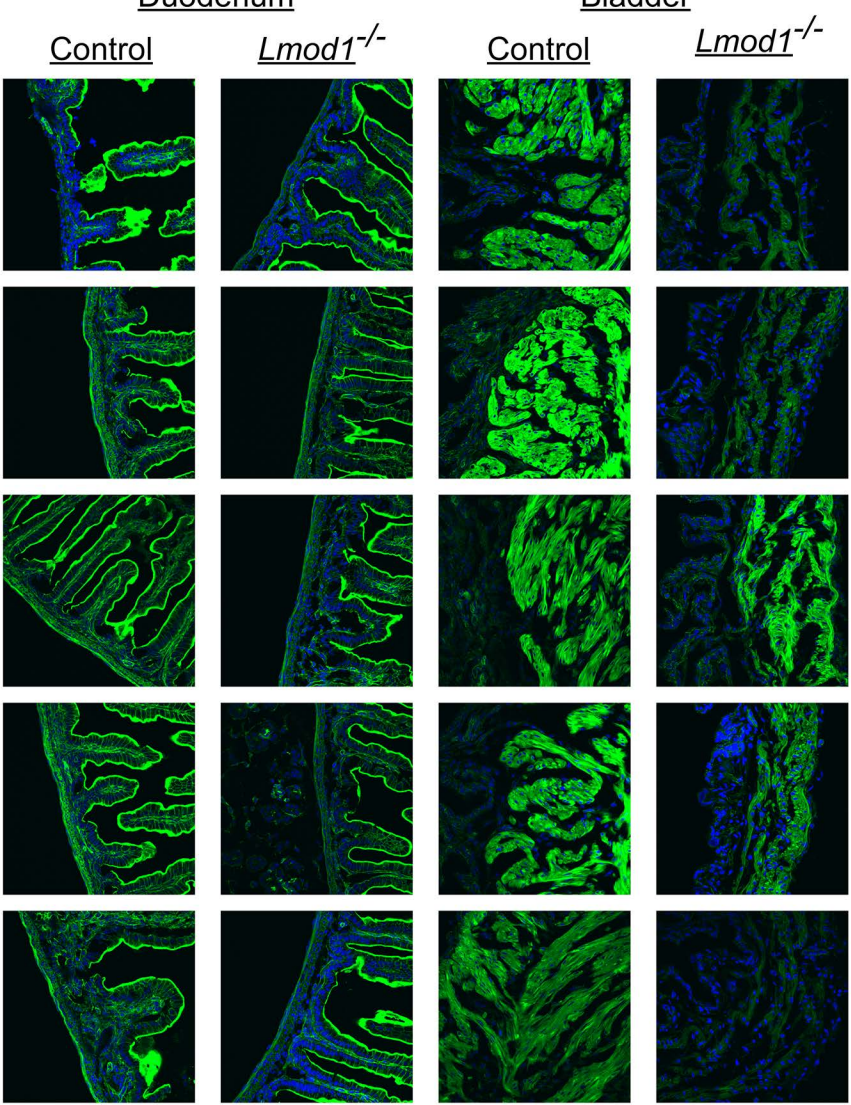
Duodenum
Bladder
Control
Lmod1-/-
Control
Lmod1-/-

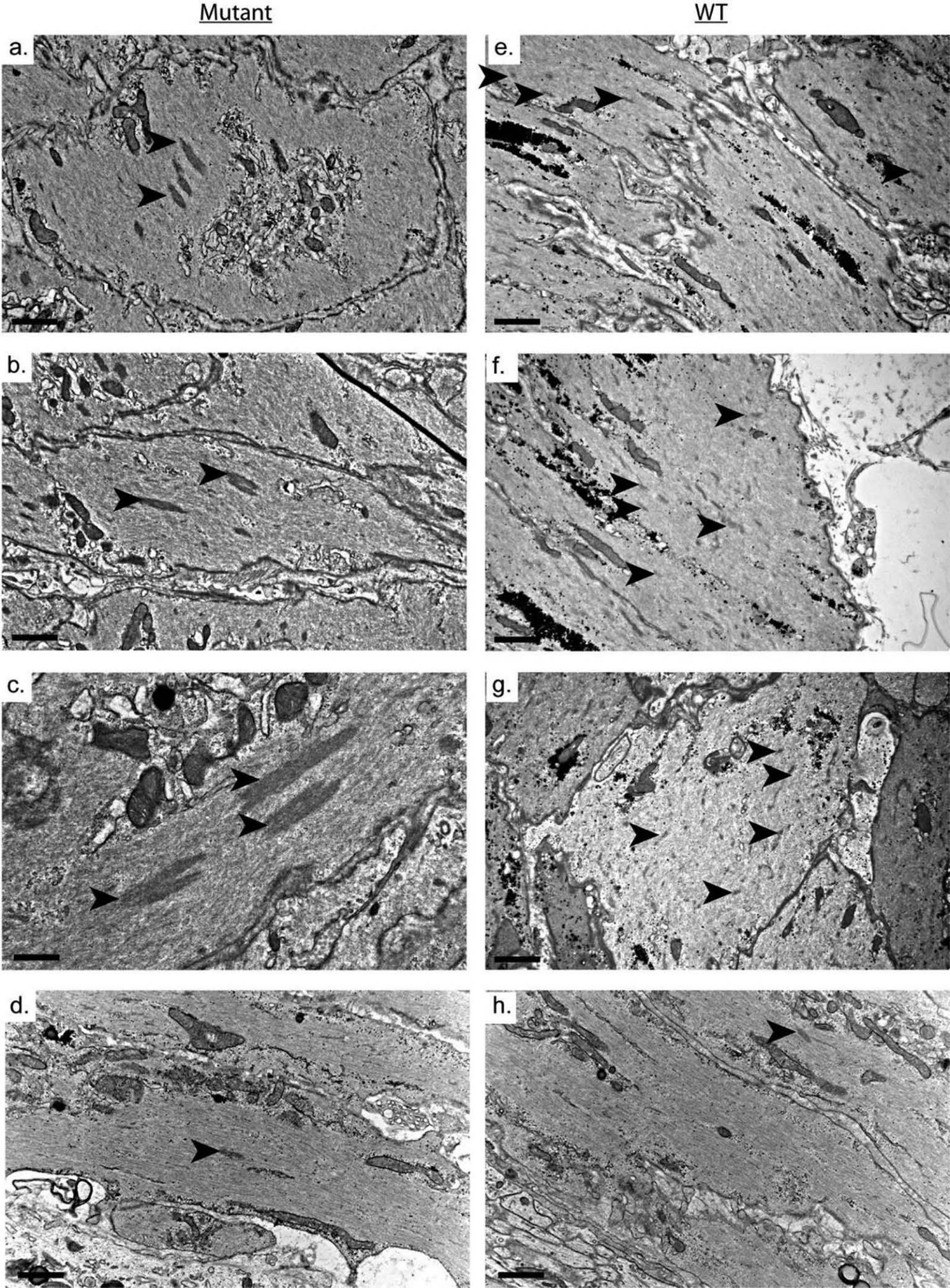
Mutant
WT
a.
e.
b.
f.
c.
g.
d.
h.

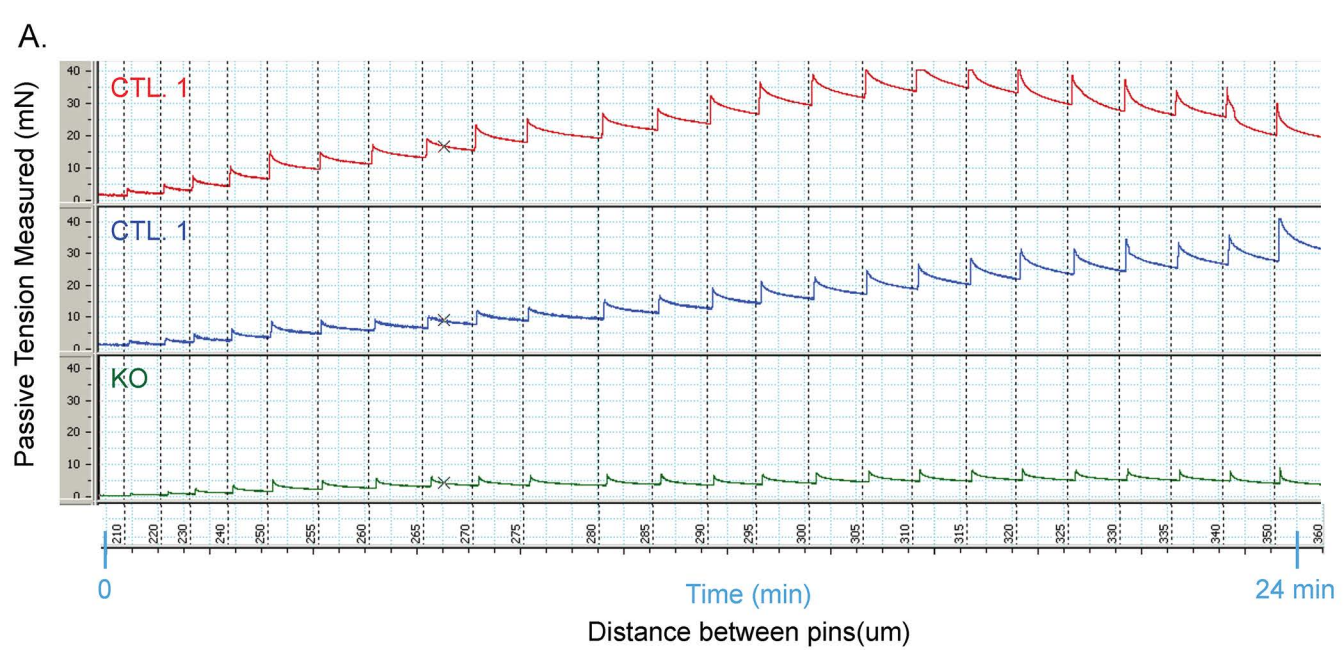
A.
Passive Tension Measured (mN)
CTL. 1
CTL. 1
KO
0
Time (min)
24 min
Distance between pins(um)

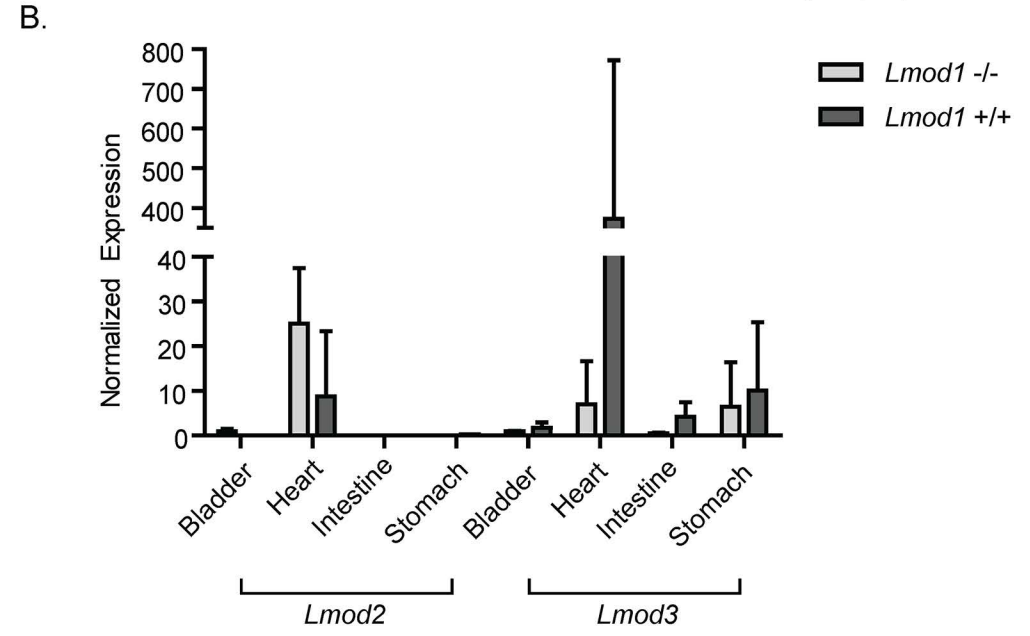
B.
Normalized Expression
Lmod1 -/-
Lmod1 +/+
Bladder
Heart
Intestine
Stomach
Bladder
Heart
Intestine
Stomach
Lmod2
Lmod3

Supplemental Table 1. Runs of homozygosity likely to be IBD

Region	Region Length	Cytoband Location	Genes	Recessive variants	Homozygous deleterious variants
chr1:143,343,508-145,535,118	2191610	q21.1	55	0	
chr1:173,370,927-174,796,005	1425078	q25.1	30	0	
chr1:193,573,186-210,528,162	16954976	q31.2 - q32.2	212	12	NM_012134.2:c.1108C>T NM_001185156.1:c.541T>G
chr1:248,058,844-249,250,621	1191777	q44	41	0	
chr1:39,434,967-40,549,847	1114880	p34.3 - p34.2	28	0	
chr10:95,863,499-97,045,599	1182100	q23.33 - q24.1	16	0	
chr12:33,710,632-35,800,000	2089368	p11.1 - q11	1	0	
chr13:20,806,399-22,561,134	1754735	q12.11	23	1	
chr13:96,306,895-97,414,036	1107141	q32.1	7	0	
chr15:76,540,526-77,848,747	1308221	q24.2 - q24.3	15	0	
chr16:46,450,037-48,939,622	2489585	q11.2 - q12.1	25	0	
chr2:119,938,409-120,962,478	1024069	q14.2	13	0	
chr2:87,375,359-90,240,473	2865114	p11.2	31	0	
chr2:95,395,757-115,363,347	19967590	q11.1 - q14.1	270	4	NM_153836.3:c.442-5G>A
chr3:16,785,031-18,119,015	1333984	p24.3	6	0	
chr3:3,352,620-5,243,227	1890607	p26.2 - p26.1	11	0	
chr4:8,660,540-9,914,140	1253600	p16.1	34	0	
chr7:32,513,692-33,555,034	1041342	p14.3	19	0	
chr8:0-4,852,787	4852787	p23.3 - p23.2	32	1	
chr8:125,828,810-128,307,073	2478263	q24.13 - q24.21	39	1	
chr8:4,941,482-8,122,303	3180821	p23.2 - p23.1	60	0	
chr8:85,664,141-86,847,889	1183748	q21.2	15	0	

Included are Runs of homozygosity larger than 1 Mb, containing ≥ 50 consecutive probes. These regions are heterozygous in the parental samples and likely to be identical by descend. Most of the recessive variants (MAF ≤ 1%) are predicted to be benign, except the variants depicted in the last column. Recessive variants are depicted in table 2

Supplemental Table 2. Homozygous recessive variants in putative IBD regions

Chr.	Start	Ref	Genotype	ExAC allele frequency	Gene	Type	Location	Effect	Exon	HGVS cDNA-level	HGVS protein-level	CADD PHRED
1	200974176	G	A A		*KIF21B*	snp	intronic		6	NM_001252100.1:c.733-115C>T		2.719
1	201038809	G	A A		*CACNA1S*	snp	intronic		18	NM_000069.2:c.2361-80C>T		3.588
1	201453417	C	T T		*CSRP1*	snp	UTR3		6	NM_001193571.1:c.*424G>A		6.002
1	201869033	G	A A		*LMOD1*	snp	exonic	stopgain	2	NM_012134.2:c.1108C>T	p.Arg370*	35
1	202156089	A	T T	0.001243781	*PTPRVP*	snp	ncRNA_intronic		18	NR_002930.2:c.3407-42A>T		3.909
1	204192659	G	A A	0.008624843	*PLEKHA6*	snp	exonic	nonsynonymous	22	NM_014935.4:c.3086C>T	p.Ala1029Val	13.13
1	204426534	T	C C		*PIK3C2B*	snp	intronic		10	NM_002646.3:c.1713+322A>G		9.315
1	207075619	A	C C		*IL24*	snp	intronic		6	NM_001185156.1:c.540+202A>C		0.266
1	207076321	T	G G	0.003566428	*IL24*	snp	exonic	nonsynonymous	7	NM_001185156.1:c.541T>G	p.Leu181Val	22.6
1	207078220	T	C C		*FAIM3*	snp	UTR3		8	NM_005449.4:c.*144A>G		9.955
1	207086885	G	A A		*FAIM3*	snp	intronic		2	NM_005449.4:c.373+219C>T		4.494
1	207133613	A	G G		*FCAMR*	snp	intronic		6	NM_001170631.1:c.1454+154T>C		3.249
2	96940649	T	C C		*SNRNP200*	snp	UTR3		45	NM_014014.4:c.*101A>G		4.171
2	102000169	C	T T		*CREG2*	snp	intronic		2	NM_153836.3:c.442-5G>A		8.603
2	102636342	G	A A		*IL1R2*	snp	intronic		5	NM_004633.3:c.688+68G>A		5.461
2	105897274	A	T T		*TGFBRAP1*	snp	intronic		6	NM_004257.5:c.1122-94T>A		3.669
8	1719112	C	T T		*CLN8*	snp	UTR5		2	NM_018941.3:c.-109C>T		8.105
8	126059429	T	C C	0.0000165	*KIAA0196*	snp	intronic		20	NM_014846.3:c.2504+20A>G		0.989
13	21296049	G	A A	0.001284481	*IL17D*	snp	exonic	nonsynonymous	3	NM_138284.1:c.565G>A	p.Ala189Thr	8.397

All Homozygous recessive variants with an MAF below 1% in putative IBD regions.

Supplemental Table 3. Off target sites of gRNAs and CRISPResso result

gRNA	Chromosome Coordinate	Primer	Primer Sequence	Mismatch positions Sequence	Location	Nearest Gene	Percent indels from CRISPResso
1	chr2:-168304560	Forward	TTTCTTCTTCCAACAGCGTTTC	2:4:8:19 CTACAGTGGCTAAGTACCCGTGG	3'utr	*Nfatc2*	0.4%
		Reverse	GGTCCTGACCACAAAGTCATA				
1	chr2:+119860458	Forward	CAAACCTGCCCAGTCTACAT	1:4:10:19 TCAGAGTAGTTAAGTACCAGTGG	intron	*Pla2g4b*	ND
		Reverse	CTTCCTTCTCCCAGACACTTC				
1	chr2:+155459613	Forward	TGGTGACAGGAAGAGTGGA	5:6:8:20 CCAACCTGGCTAAGTACCGCAAG	exon	*Myh7b*	0.3%
		Reverse	CACTCCTTGTGCTAAGAGATGAA				
1	chr3:+81759039	Forward	CTTCTTGCCTTCTTCCCTCTG	9:12:20 CCAAAGTAACTCAGTACCGTTGG	3'utr	*Ctso*	0.0%
		Reverse	CCGTTTCTTTACCCTCCATGAT				
1	chr11:-69611753	Forward	GGTTCTCTAAGGGTGAGTGTAAG	4:8:11:13 CCACAGTGGCCATGTACCGGGAG	exon	*Fgf11*	0.6%
		Reverse	GCTCAGGGCATGTGTGT				
1	chr7:+36220567	Forward	TGGTCCTTCTGTCTCCTTAGAT	1:7:12:19 GCAAAGCAGCTCAGTACCAGAAG	exon	*Cep89*	ND
		Reverse	GCTCCCGCACTTACCTTT				
1	chr5:+44105813	Forward	TACTGGCTATGCACCAAAGG	4:11:19:20 CCACAGTAGCCAAGTACCTTCAG	exon	*Cc2d2a*	1.0%
		Reverse	CCATCTTACAATCGTGGCTCT				
1	chr10:-94052876	Forward	CCAGGCAATTAGGTCTGGATT	9:14:17:18 CCAAAGTAACTAATTATTGGGAG	3'utr	*Tmc33*	0.5%
		Reverse	CTTGTGTTGTCTGTTGGTGTTC				
1	chr6:+32136129	Forward	GGGAAGCAAGCCAGTAAAGA	1:10:19 GCAAAGTAGTTAAGTACCTGCAG	intron	*Plxna4*	0.0%
		Reverse	CTGCATCACCATCAGGAAAGA				
1	chr9:+40970879	Forward	ATAGAACGTGGTGTGGAAGTG	1:06:13 TCAAAATAGCTAGGTACCGGAGG	intergenic	*Ubash3b*	ND
		Reverse	ACTTCCACACTAAACTGGGTGT				

2	chr15:+60655990	Forward	GGGAGGGAAGGAAATAGAAACT	3:06:07 GGACTAGACTCACCTGCCGCAAG	intron	*Fam84b*	1.0%
		Reverse	GCGAACTCGCCCTAGAAG				
2	chr12:+85262753	Forward	TACCTTCCCAGCTCCAACT	1:3:5:6 CGCCCGCACTCACCTGCCGCTGG	intron	*Numb*	ND
		Reverse	GGACAGGAAGAGTCAACCAATC				
2	chr6:+85290322	Forward	CCAAATAGAGGAGACCCTTACC	4:5:6:8 GGTGGACGCTCACCTGCCGCTGG	intron	*Rab11fip5*	0.2%
		Reverse	GGCCCTTGACCTCTTCTTC				
2	chr8:-123093143	Forward	AGGAGGACAGATAGACAGACTT	8:09:12 GGTCTTCCTTCTCCTGCCGCAGG	exon	*Gse1*	0.5%
		Reverse	GTGCCCAGCCTCATCTC				
2	chr1:-174475299	Forward	GCTCTTCCAGCTTCTGTTTCT	4:5:10:20 GGTTCTCACGCACCTGCCGTCGG	exon	*Cfap45*	0.0%
		Reverse	TGTGGACCTTGAAGCATGAC				
2	chr11:+54864689	Forward	CTTTCTGACTCCCAAGGAAAGA	5:9:10:12 GGTCCTCAACCTCCTGCCGCAGG	exon	*Ccdc69*	ND
		Reverse	ACTGTGCCAAGAGTGAGTG				
2	chr5:-121812464	Forward	CCTACCTCACCTTGTTCTTGTT	2:7:10:19 GCTCTTTACACACCTGCCACAGG	exon	*Gm15800*	0.7%
		Reverse	AGCTAGGGTCAGCATCTCA				
2	chr19:-46384378	Forward	CAGGCATGTGCAATATTTGGG	6:10:18 GGTCTGCACCCACCTGCAGCAGG	exon	*Nfkb2*	0.9%
		Reverse	GCAGATAGCCCACGTCATTTA				
2	chr15:-83161031	Forward	AGAGAGGGAGAGAGAGAGAGA	1:3:8:18 TGGCTTCTCTCACCTGCTGCAGG	exon	*Arfgap3*	ND
		Reverse	CAGGAGACCACAGGACATTG				
2	chr2:-167433844	Forward	GGTGAGGAATTCAGGGCTTC	3:5:6:19 GGACCACACTCACCTGCCACCAG	3'utr	*Ube2v1*	0.3%
		Reverse	GGCCTTTCTCTAGGCATCTTT				
3	chr6:-50334908	Forward	GCTTCACCTAAGGGACTTGTAG	4:08:18 TCCTGGTAGAATGAGCCTGATGG	intron	*Osbp13*	1.1%
		Reverse	AGGTCTTACTGACTCCCACATA				

3	chr2:+120960142	Forward	GGCTGTCCTAGAACTCACTTTG	4:5:8:17 TCCTTGTGGAATGAGCTCGAGAG	intergenic	*Lcmt2*	0.6%
		Reverse	GAGCGTCCTTAGGGAGATAGAT				
3	chr18:+16761798	Forward	AGAGATGGTCTGAGCAAAGATAAG	3:5:11:12 TCACAGTTGACAGAGCCCGAGGG	intron	*Cdh2*	ND
		Reverse	CAGAGGGAGTAATGTTGGGATAAG				
3	chr19:+15937358	Forward	GAGGTCTGTGTGCAAAGGT	3:5:7:19 TCTCTGATGAATGAGCCCCACAG	intergenic	*Psat1*	0.4%
		Reverse	GCTTCGGTTACTGCTGAGTT				
3	chr3:-60477413	Forward	CACACTGATGCCCAGGATAAA	4:5:8:18 TCCAAGTGGAATGAGCCAGAAAG	intergenic	*Mbnl1*	ND
		Reverse	ACAGAGAAGTTACATGCAGAGAAG				
3	chr9:-57442270	Forward	TTGATCTGCTCCTTCAGGTATTC	5:10:12:20 TCCCTGTTGTAGGAGCCCGGCAG	intron	*Ulk3*	ND
		Reverse	CTCAGGTCTGTGGGACATAAATAG				
3	chr2:-148578529	Forward	CATATAGTGGAGAGAAGCTCTTGG	4:15:19 TCCTGGTTGAATGATCCCCATAG	intron	*Cst11*	0.0%
		Reverse	AGTGGTTGGCACAGTTCTAC				
3	chr2:-147438139	Forward	TCAACAGAGCACAGCAGAC	4:7:8:18 TCCTGGAAGAATGAGCCAGACAG	intergenic	*Pax1*	ND
		Reverse	TTATGACAGCTTGAACCCTACC				
3	chr13:-52994868	Forward	CCGGTTTCTCAGTGTCCTTT	3:8:10:14 TCTCGGTGGCATGTGCCCGAGAG	intron	*Auh*	1.2%
		Reverse	GGGTCATTTCGCTCTGAGTT				
3	chr16:-10681231	Forward	GGTGTGAAGACAGCGACTAT	4:5:13:19 TCCTTGTTGAATTAGCCCCAAGG	intron	*Clec16a*	0.0%
		Reverse	GAGAGCAGTGGGTTGAGAAT				

Supplemental Table 4. Oligonucleotides used for RT-PCR, genotyping, gRNA, and repair template

Oligonucleotide		Sequence
Sequencing mutation in exon 2 Human *LMOD1*	Forward	GGAGGTGGCCAAGAAAGAGG
	Reverse	ATCATGAAGCCAGGGTCTCC
qRT-PCR Human *LMOD1*	Forward	GAGGCCATGCTCAACTTCTG
	Reverse	CTCTCCATTCTTGGCATCTG
qRT-PCR Human *COPS5*	Forward	CCAGGAACCATTTGTAGCAG
	Reverse	GTAGCCCTTTGGGTATGTCC
qRT-PCR Human *CLK2*	Forward	TCGTTAGCACCTTAGGAGAGG
	Reverse	TGATCTTCAGGGCAACTCG
PCR genotyping primers for deletion in exon 1 Mouse *Lmod1*	Forward	GCCCAAAGAGCTGCAGTGC
	Reverse	CTCACATCCACAGACATCTCTCTC
qRT-PCR Exon 1 Mouse *Lmod1*	Forward	TGTGGATGAAAGCAAGCAAGTG

	Reverse	AATACCTCTGATGACCTTCTCCTC
qRT-PCR Exon 2 Mouse *Lmod1*	Forward	CTGCCATCCGTTCTAGCAAC
	Reverse	CAAGAGTCTGGGCAGTCATG
qRT-PCR Mouse *Gusb*	Forward	CATCAGAAGCCGATTATCCAGAG
	Reverse	TGTTTCCGATTACTCTCAGCG
2-component CRISPR gRNA1 (exon1)		CCAAAGTAGCTAAGTACCGG
2-component CRISPR gRNA2 (exon 1)		GGTCTTCACTCACCTGCCGC
2-component CRISPR gRNA3 (exon 1)		TCCCGGTTGAATGAGCCCGA
3-component CRISPR (CArG boxes)		AAACTGCTCTGTACTAAATT
ssoligo for 3-component CRISPR editing of CArG boxes		TCCTGCGGCTTCTGCCAGCCTTTGCATTTTTCTCTTTTTCTCAT TGCGTGGCCCCCTTGTGGGTAAAAGGCTAAACTGCTCTGTAGG GAATTTGGTCACGCAGCGCTCCAAGATTCCCTGGAATGTCCTC